

20-Gb/s silicon optical modulators for the 2 μm wavelength band

Wei Cao[†], David J. Thomson, Milos Nedeljkovic
Shaif-ul Alam, Junjia Wang, Frederic Gardes
Graham T. Reed, Goran Z. Mashanovich
Optoelectronics Research Centre, University of Southampton
Southampton, United Kingdom
[†]: wei.cao@soton.ac.uk

Callum G. Littlejohns, Mohamed Said Rouifed
Silicon Technologies Centre of Excellence
Nanyang Technological University
Singapore

Abstract—We demonstrate silicon-on-insulator based high speed modulators working at a wavelength of 1950 nm. The carrier-depletion Mach-Zehnder interferometer modulator operates at a data rate of 20 Gbit/s with an extinction ratio of 5.8 dB and modulation efficiency ($V_{\pi}L_{\pi}$) of 2.68 Vcm at 4 V reverse bias.

I. INTRODUCTION

We are facing the risk of a “capacity crunch” as we are approaching the theoretical capacity limit of conventional single mode fibres (SMFs)[1]. Hollow-core photonic bandgap fibres (HC-PBGF) show lower predicted loss and nonlinearity than the best SMF. Its lowest loss is calculated at 2 μm [2], which opens a new wavelength band for telecommunications [3]. In the meantime, such a wavelength coincides with the gain window of thulium-doped fibre amplifiers (TDFA), and in addition, at this wavelength one can take advantage of the integration capability of silicon photonics. While a 20 Gbit/s silicon photonics based detector at 2 μm has been demonstrated [4], there have been few modulators. Previously only IBM has shown a 3 Gbit/s carrier injection SOI modulator at 2 μm . In this paper we present state of the art silicon photonics based high speed modulators operating at up to 20 Gbit/s.

II. SIMULATION & DESIGN

Silicon is predicted [5] to exhibit a stronger free carrier effect at 2 μm than at both 1300 nm and 1550 nm. We have designed Mach-Zehnder interferometer (MZI) modulator using PN junction phase shifters. The phase shifter response is analysed by a combination of electrical device simulation using Silvaco TCAD tools and optical device simulation using a MATLAB based waveguide mode solver [6].

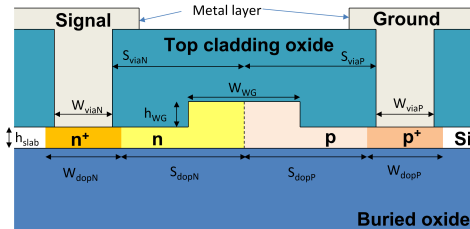


Fig. 1: Cross section of the phase shifter for MZM and ring modulator.

Figure 1 shows a schematic of the cross section of the phase shifter in the MZI modulators and ring modulators. Both types of modulator share a similar cross section design but the dimensions are different. The MZI modulators exploit the carrier depletion effect. Devices are fabricated on 220 nm SOI wafers with a 2 μm buried oxide (BOX) layer. The silicon rib waveguide is 550 nm wide (W_{WG}) and etched by 90 nm in the slab region (h_{WG}). The PN junction position is in the centre of the waveguide and the highly doped regions are 1.125 μm (S_{dopN}) and 1.025 μm (S_{dopP}) away from the junction. The target doping concentrations in the simulation are $3\text{e}17\text{ cm}^{-3}$, $8.5\text{e}17\text{ cm}^{-3}$, $1\text{e}20\text{ cm}^{-3}$ and $1\text{e}20\text{ cm}^{-3}$ for the n, p, n+, and p+ regions respectively.

Figure 2 is an optical microscope image of the core of the MZI modulator. The device is fabricated by IME in a multi-project wafer (MPW) run with customised doping concentrations. The device is designed with Y-splitters in the MZI and it uses butt coupling, so that we are able to test the device under both 1550 nm and 1950 nm light.

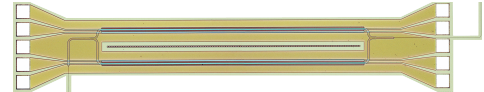


Fig. 2: Optical microscope image of the MZI modulator.

III. EXPERIMENTAL SETUP

As most 1300/1550 nm equipment is incompatible with the 2 μm wavelength, expanding the measurement capability to 2 μm requires some bespoke 2 μm equipment: an EOT ET-5000 high speed 2 μm InGaAs detector (rated bandwidth of >12.5 GHz and peak responsivity of 1.3 A/W at 2000 nm); an amplified Thorlabs low speed 2 μm InGaAs detector; Thorlabs SM2000 silica fibres; and a Thorlabs TLK-L1950R tunable laser (1890 nm - 2020 nm). We have also used a TDFA to increase the optical power (about 13 dB gain), similar to [7]. During the high speed testing, a pseudorandom binary sequence generator (PRBS) is used to generate a bit sequence. The high speed electrical signal is then amplified and applied to the device with an RF probe. A bias tee is used to combine DC bias and high speed RF signal.

Compared to the conventional 1300/1550 nm setup, there are limitations in the 2 μm system. The high speed detector

had a nominal bandwidth of $>12.5\text{GHz}$, limiting the speed at which we could measure the modulator to around 20 Gbit/s and with reduced extinction ratio. A signal faster than 20Gbit/s cannot operate with the detector.

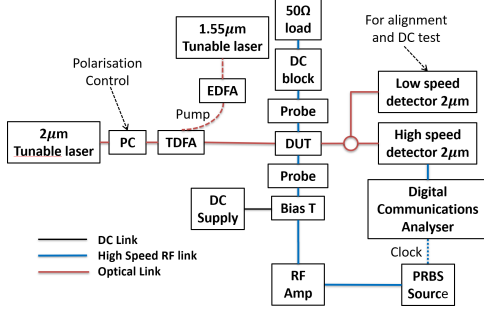


Fig. 3: High-speed RF measurement set up for $2\text{ }\mu\text{m}$ wavelength modulator.

IV. RESULTS AND ANALYSIS

We tested and confirmed that the device transmits and modulates at both 1550 nm and 1950 nm . The modulation efficiency ($V_{\pi}L_{\pi}$) at a reverse bias of 4 V is 2.02 Vcm at 1550 nm and 2.68 Vcm at 1950 nm . The experimental phase shift for the measured MZM that comprises a 1.5 mm long phase shifter is shown in figure 4. It can be seen that the response agrees reasonably well with the simulation predictions for both wavelengths.

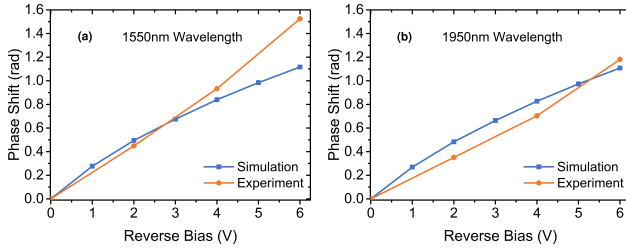


Fig. 4: Experimental and simulated phase shift for a MZI modulator with 0.15 cm long phase shifter. (a) Phase shift at 1550 nm . (b) Phase shift at 1950 nm .

The high speed RF characterization is performed by applying a DC bias of -2.5 V and an amplified highspeed $2^7 - 1$ pseudorandom-bit-stream OOK signal with a peak-to-peak amplitude of 4 V . At 1950 nm , an open eye is obtained at 8 Gbit/s with an extinction ratio of 7.6 dB and 20 Gbit/s with extinction ratio of 5.8 dB , as shown in figure 5. At 1550 nm , the device modulates at 20 Gbit/s with an extinction ratio of 10.3 dB , as in figure 6(a), and 30 Gbit/s with an extinction ratio of 7.1 dB , as in figure 6(b).

According to the simulation, the MZM should give similar RF performance for both 1550 nm and 1950 nm wavelengths. The power budget of the system however is lower at 1950 nm , which renders the eye diagram at 1950 nm noisier than at 1550 nm . The insertion loss of the device at 1950 nm is measured as

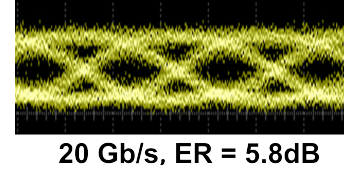


Fig. 5: Eye diagram for MZI modulator at data rate of 20 Gb/s at 1950 nm wavelength. Extinction ratio is 5.8 dB .

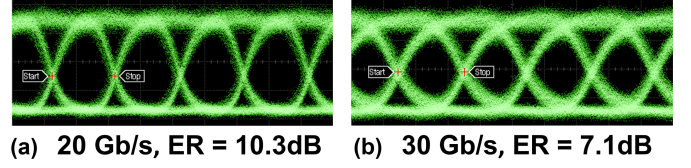


Fig. 6: Eye diagram for MZI modulator at 1550 nm wavelength. (a) Data rate is 20 Gb/s , Extinction ratio is 10.3 dB . (b) Data rate is 30 Gb/s , Extinction ratio is 7.1 dB .

13 dB which is significantly higher than was measured at 1550 nm (4 dB). The difference can be attributed to loss from metal absorption in areas where the waveguide passes directly below the metal layer. The vertical separation between the top of the Si waveguide and the bottom of the metal layer is only 600 nm and because the optical mode at 1950 nm is substantially larger, there is greater overlap with the metal.

Because of the bandwidth limit of the detector we were unable to obtain an eye diagram for data rates greater than 20 Gbit/s at $2\text{ }\mu\text{m}$ wavelength, but since the bandwidth of the PN junction should be very similar at both wavelengths, we expect that the modulator can operate at higher data rates.

ACKNOWLEDGMENT

EPSRC (MIGRATION EP/L01162X/1, National Hub in High Value Photonic Manufacturing EP/N00762X/1, CORNERSTONE EP/L021129/1); RAEng (M. Nedeljkovic fellowship RF201617/16/33); NRF (NRF-CRP12-2013-04).

REFERENCES

- [1] A. Ellis *et al.*, "Capacity in fiber optic communications-the case for a radically new fiber," in *IEEE Photonic Society 24th Annual Meeting*. IEEE, oct 2011.
- [2] E. Desurvire *et al.*, "Science and technology challenges in XXIst century optical communications," *Comptes Rendus Physique*, vol. 12, no. 4, pp. 387–416, may 2011.
- [3] R. Soref, "Group IV photonics: Enabling $2\text{ }\mu\text{m}$ communications," *Nature Photonics*, vol. 9, no. 6, pp. 358–359, may 2015.
- [4] J. J. Ackert *et al.*, "High-speed detection at two micrometres with monolithic silicon photodiodes," *Nature Photonics*, vol. 9, no. 6, pp. 393–396, may 2015.
- [5] M. Nedeljkovic *et al.*, "Free-carrier electrorefraction and electroabsorption modulation predictions for silicon over the $1\text{--}14\text{-}\mu\text{m}$ infrared wavelength range," *IEEE Photonics J.*, vol. 3, no. 6, pp. 1171–1180, dec 2011.
- [6] A. B. Fallahkhair *et al.*, "Vector finite difference modesolver for anisotropic dielectric waveguides," *Journal of Lightwave Technology*, vol. 26, no. 11, pp. 1423–1431, jun 2008.
- [7] Z. Li *et al.*, "Thulium-doped fiber amplifier for optical communications at $2\text{ }\mu\text{m}$," *Optics Express*, vol. 21, no. 8, p. 9289, apr 2013.